MPC Based Trajectory Tracking Simulation of Membrane Wall Welding Gantry Robot Arm

Zijian Zhao[1, 2], Changqing Liu[1], Ping Yang[1, *], Pengyuan Zou[1, 2]

[1]Department of Mechanical Materials, Science and Technology College of Nanchang Hangkong University, Jiujiang 332020, China

[2]Jiangxi Key Laboratory of Forming and Joining Technology for Aerospace Components, Nanchang 330088, China

Abstract: *Purpose* - Through a series of iterative processes, the proposed method allows the manipulator to get as close as possible to the desired path under joint constraints with high accuracy and short computation time. To meet the urgent need for accuracy and stability in the membrane wall welding process. *Design/methodology/approach* - This study focuses on the potential of model predictive control (MPC) to improve the ability of robotic systems to accomplish complex welding tasks. First, a gantry arm model suitable for membrane wall welding was developed for kinematic calculations. Extensive simulation tests were then conducted to investigate the accuracy and feasibility of MPC in accomplishing membrane wall welding tasks and its efficiency in resolving kinematic constraints. Finally, parameters such as trajectory accuracy and system responsiveness were also examined. *Findings* - The MPC approach significantly improved the trajectory tracking process for membrane wall welding, and the control system demonstrated high accuracy, efficiency, and adaptability, especially in nonlinear multiple-input. These multiple-output redundant robotic welding scenarios contribute to the development of more complex, accurate, and reliable robotic welding systems. *Originality/Value* - Through a series of iterative processes, the proposed method enables the gantry manipulator to get as close as possible to the desired paths under the welding structure and the motion degrees of freedom constraints, with high accuracy and fast convergence speed. *Ethical Compliance*: All procedures performed in studies involving human participants were in accordance with the ethical standards of the institutional and/or national research committee and with the 1964 Helsinki Declaration and its later amendments or comparable ethical standards.

Keywords: Model Predictive Control; Membrane Wall Welding; CoppeliaSim; Trajectory Tracking Control; Gantry with Robot Arm

DOI: 10.57237/j.mse.2026.02.001

1 Introduction

With the rapid development of automation and intelligent manufacturing technologies, robotic-arm automated welding is playing an increasingly important role in industrial production. To meet the needs of various complex application scenarios and improve welding quality and production efficiency, the study of high-precision and high-stability robotic arm control technology has become crucial. The combination of the gantry and robotic arm is an essential industrial machinery combination that is widely used in

Funding: The Jiangxi Key Laboratory of Forming and Joining Technology for Aerospace Components (No: EL202280319); Science and Technology Research Project of Jiangxi Provincial Department of Education (No: GJJ218716 and No: GJJ2204316); Technology Research Project of Jiangxi Province Education Department (Grant No. S20231343310); Nanchang Hangkong University Science and Technology College Student Innovation and Entrepreneurship Program (No: S20231343320).

*Corresponding author: Ping Yang, yp_829@163.com

Received: 21 April 2026; Accepted: 20 May 2026; Published Online: 8 June 2026

the assembly, product sortation, shipping, welding, and other industrial fields [1-4], especially for boiler membrane wall welding operations are more widely used. Stable and precise planning of the trajectory of this mechanical structure is crucial for the efficiency, safety, and stability of industrial production processes [5, 6]. However, there have been some challenges in the industrial application of this combination, such as the complexity and uncertainty of the robot arm movement [7] and the problem of priority allocation of cooperative control between the robot arm and gantry [8]. therefore, the accurate prediction and control of the motion trajectory is a complex problem in the field of robotics research.

Control accuracy is critical for operational efficiency and safety in fields such as energy production and advanced manufacturing. Particularly in specialised applications, such as membrane wall welding, the integration of gantry systems [9, 10] and the adoption of Model Predictive Control (MPC) hold transformative promise [11]. With safety being paramount in welding operations, Ma *et al.* highlighted the reduced risk profile of gantry systems, emphasising their potential to reduce manual errors [12]. Wang *et al.* [13] further extended this discourse, positing that the structured movement of gantries provides an ideal platform for integrating automation tools, thereby refining the welding process.

In scientific research concerning membrane wall welding, Model Predictive Control (MPC) has demonstrated considerable advantages over traditional control methods such as PID, adaptive control, and fuzzy logic controllers [14-16]. MPC's unique predictive capability of MPC allows it to anticipate the future state of the welding process, thus enabling proactive and precise adjustments. This feature is particularly advantageous for the complex dynamics of membrane wall welding, where conditions and requirements are prone to rapid fluctuations [17-19], the predictive nature of MPC can potentially address these challenges by adapting welding parameters to material variations in real-time. Moreover, MPC's robustness and adaptability of MPC to system changes and external disturbances ensures greater control accuracy and stability [20, 21]. Additionally, MPC can seamlessly integrate process constraints into its control strategy, which is a crucial feature for maintaining safe and efficient welding operations.

This paper presents a novel approach to the challenges of motion planning, joint constraints, and obstacle avoidance in robotic welding using a gantry robotic arm. Initially, the attitude of the gantry robotic arm was described using Euler angles. Subsequently, a predictive control model was developed that considered the mechanical characteristics of the membrane wall gantry robotic arm. The effectiveness of our approach in achieving point-to-point motion during welding was demonstrated through MATLAB simulations. Finally, we employed CoppeliaSim to simulate the entire membrane wall welding process and analysed the efficacy and accuracy of the MPC strategy.

The structure of this paper is as follows. Section 2 introduces the background of membrane wall welding. Section 3 describes the mathematical model of the membrane-wall welding robot. Section 4 presents the design of algorithms for the predictive control of the model and optimisers to handle constraint and tracking problems. Section 5 validates the experiments through a combined simulation using CoppeliaSim and MATLAB.

2 Introduction of Membrane Wall Welding

Welding operations are ubiquitous in the power station boiler industry, with a vast number of welding operations on anisotropic membrane water condensation walls ("membrane walls") [22].

This industrial structure is a tube and flat steel welded tube screen, and several groups of tube screens together form a membrane wall with the role of absorbing the high-temperature flame or flue gas generated by the radiation heat in the furnace chamber to reduce the temperature of the furnace wall and play a protective role, with the advantages of being a simple structure, saving steel, providing insulation, and having a better airtight effect.

As the membrane wall generally exists in many complex anisotropic space structures, both vertical and horizontal, the system is variable, so the issue to be resolved between the membrane wall and the partition is the complexity of its spatial characteristics. Figure 1 shows the simulation model environment built by the authors in CoppeliaSim based on an actual welding scenario to verify the effectiveness of the MPC motion model in terms of control.

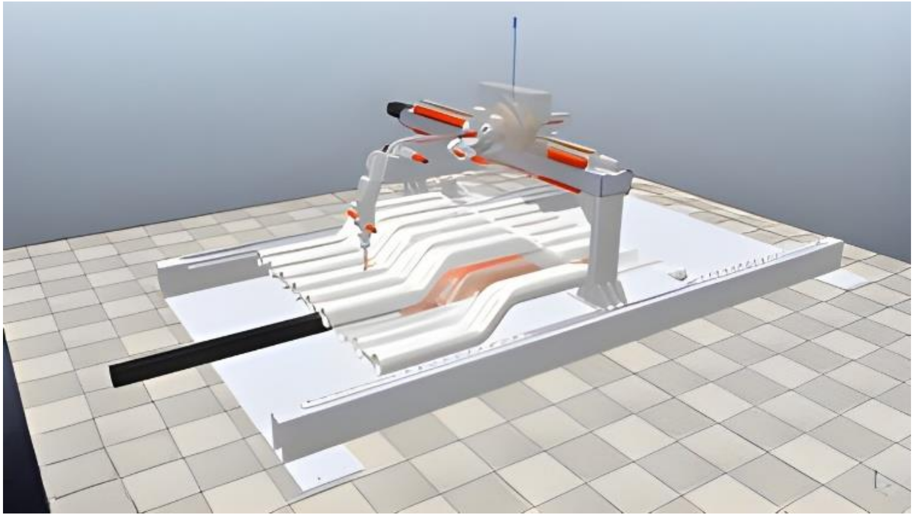

Figure 1 The Robot Arm with Gantry

This study uses a two-axis truss structure in conjunction with the movement of a five-axis robotic arm, reducing the limitations of the degrees of freedom of the welding robotic arm and allowing it to be used in specific application scenarios, such as shipbuilding, tank fabrication, and membrane wall welding.

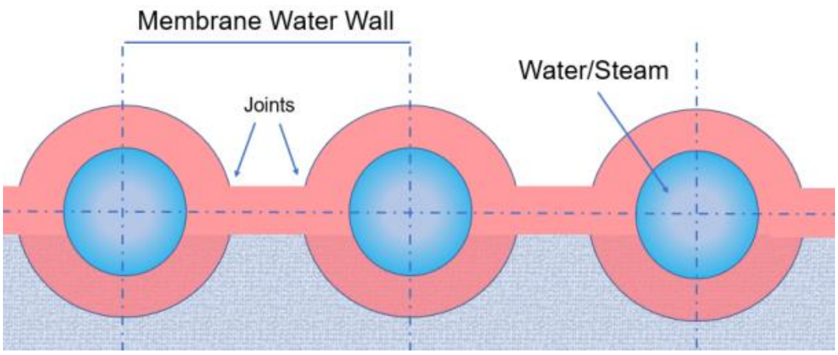

(a)

(b)

Figure 2 a): Membrane Wall Theoretical Model; b) Membrane Wall Space Geometry

Figure 2(a). shows a theoretical model of a membrane wall that describes the welding joints' exact location and the membrane wall's physical structure. To reflect the unique characteristics of the membrane wall welding space structure, this study used a Ω-shaped space structure and cross-section, as shown in Figure 2(b).

3 Wilding Robot Model

Accurate control of the welding torch is required to automate the entire membrane wall weld, as the accuracy of predictive control based on the state MPC equation is easily influenced by the accuracy of the kinematic model. Achieving accurate control requires kinematic analysis to provide theoretical support for subsequent membrane wall weld trajectory planning.

The control output is given by the terminal attitude, and the control input is given by seven joint variables. Therefore, we use the relationship between them to construct a mathematical model. First, the coordinates of the robot joints were established, as shown in Figure 3. Subsequently, a modified Denavit-Hartenberg model was built based on the coordinates. The modified D-H parameters are presented in Table 1.

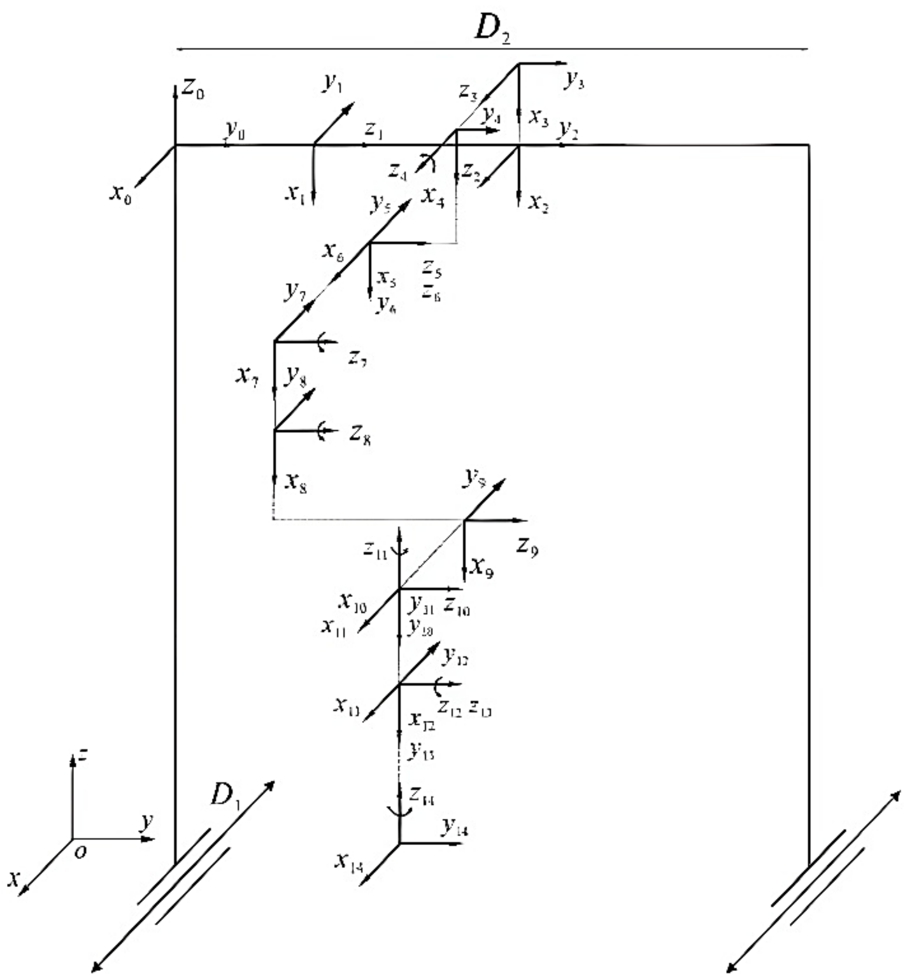

Figure 3 Kinematic coordinate system

Table 1 D-H Model of Robot

i	α_{i-1}	a_{i-1}	θ_{i-1}	d_{i-1}
1	-90°	0	90°	D_2
2	90°	0	0	D_1
3	0	-0.21	0	0
4	0	0	$-\theta_4$	0.695
5	-90°	0.15	0	-0.1
6	0	0.307	-90°	0
7	0	0	$-\theta_5$+90°	0
8	0	0.58	$-\theta_6$	0
9	0	0.3	0	0.179
10	0	0.255	-90°	0
11	90°	0	$-\theta_7$	0
12	-90°	0.43	$-\theta_8$+90°	0
13	0	0	-90°	0
14	90°	0	0	-0.515

As shown in the table, D_1 and D_2 are the translational motion joint variables in the gantry. $\theta_4 - \theta_8$ are the rotational joint variables of the robotic arm. The following equations were used for the forward motion calculations.

$$
{}_{i}^{i-1}T = \begin{pmatrix} \cos\theta_i & -\sin\theta_i & 0 & a_{i-1} \\ \sin\theta_i \cos\alpha_{i-1} & \cos\theta_i \cos\alpha_{i-1} & -\sin\alpha_{i-1} & d_i \sin\alpha_{i-1} \\ \sin\theta_i \sin\alpha_{i-1} & \cos\theta_i \sin\alpha_{i-1} & \cos\alpha_{i-1} & d_i \cos\alpha_{i-1} \\ 0 & 0 & 0 & 1 \end{pmatrix}
$$

$$
T = {}_{1}^{0}T \cdots {}_{i}^{i-1}T \cdots {}_{14}^{13}T = T(\theta)
$$

4 Description of Terminal Posture

First, a base point coordinate system was established in the 3D model, and then the posture and translation transformations were combined to create a complete representation of the relative poses at the end of the welding gun. The Euler angles were chosen to represent the relative poses in the 3D space. The matrix formula for the Euler angles is shown as (1):

$$\left(\alpha,\beta,\gamma,p_x,p_y,p_z\right) \tag{1}$$

where indicates the angle of positional deflection at the end of the torch from the initial coordinate system, and the vector represents the value of the coordinates from any point in the coordinate system to the coordinate system S_1. The relationship between the Euler's angle and the rotation equation is shown as (2):

$$^{A}\tilde{p}=\begin{pmatrix} ^{A}R_B & t \\ 0_{1\times 3} & 1 \end{pmatrix} {}^{B}\tilde{p}={}^{A}T_B\,{}^{B}\tilde{p} \tag{2}$$

Where the Cartesian translation vector between the origin of the coordinate system is t, the change in pose is represented by an orthogonal submatrix R, and the remaining vectors are expressed in a homogeneous form. The 4×4 flush transformation is expressed in (4).

$$^{A}R_B=\begin{bmatrix} \alpha_x & \beta_x & \gamma_x & p_x \\ \alpha_y & \beta_y & \gamma_y & p_y \\ \alpha_z & \beta_z & \gamma_z & p_z \\ 0 & 0 & 0 & 1 \end{bmatrix} \tag{3}$$

5 Model Predictive Control Strategy

5.1 Predictive Model

The welding process of a membrane wall is a multistage repetitive path-tracking problem that occurs in a complex topological space. Because the problem is characterised by multiple degrees of freedom redundancy of the robot arm, multivariate, non-linearity, multiple constraints, and multi-system coupling, this study designs a constrained optimised controller. It reduces it to a point-to-point path planning problem and finally simulates the motion results of the optimised controller using simulation software.

In this system, the position and attitude of the end of the welding gun are defined as (4):

$$P=\left(x,y,z,R_x,R_y,R_z\right) \tag{4}$$

The mathematical model of a gantry robot based on a membrane wall welding robot can be defined as (5):

$$x=f(\theta) \tag{5}$$

Where $x=P$ is the final attitude of the end of the welding torch and $\theta=[L_1,L_2,\theta_1,\theta_2,\cdots,\theta_5]$ is the variable of the movement and rotation of the gantry and robot arm joints.

After deriving both ends of the equation, the state-space equation is obtained as:

$$\dot{x}=\frac{\partial f(\theta)}{\partial\theta}\cdot\dot{\theta} \tag{6}$$

As MPC is a type of sampling control, the control quantity can only be calculated according to the deviation at the sampling moment; therefore, in computer control systems, the formula must be discretised, and the discretised and simplified state-space equation is (7):

$$\begin{aligned} &x(k+1)=x(k)+T\cdot\frac{\partial f(\theta)}{\partial\theta}\cdot\dot{\theta}(k)=A\cdot x(k)+B\cdot u(k) \\ &y(k)=C_T x(k) \end{aligned} \tag{7}$$

In the above equation, A/B is the system input variable coefficient, $u(k)$ is the system input variable, $y(k)$ is the system output variable; $x(k)$ is the system state variable which is measurable in real time.

Assuming that the system input changes in M steps from moment k and remains constant thereafter, the system output state can predict the system's output state for the next P (P>=M) moments at $u(k),u(k+1),\cdots,u(k+M)$. The output state can be defined as

$$\boldsymbol{Y}(k)=\boldsymbol{F}_y\boldsymbol{x}(k)+\boldsymbol{G}_y\boldsymbol{U}(k) \tag{8}$$

where,

$$\boldsymbol{Y}(k+1)=\begin{bmatrix} y(k+1) \\ \vdots \\ y(k+P) \end{bmatrix}_{6P\times 1} \quad \boldsymbol{F}_y=\begin{bmatrix} O \\ \vdots \\ O^P \end{bmatrix}_{6P\times 6}$$

$$\boldsymbol{U}(k)=\begin{bmatrix} \dot{\theta}(k) \\ \vdots \\ \dot{\theta}(k+M-1) \end{bmatrix}_{7M\times 1}$$

$$\boldsymbol{G}_y=\begin{bmatrix} \boldsymbol{C}_T\boldsymbol{b} & 0 & 0 \\ \vdots & \ddots & 0 \\ O^{M-1}\boldsymbol{b} & \cdots & \boldsymbol{C}_T\boldsymbol{b} \\ \vdots & \ddots & \vdots \\ O^{P-1}\boldsymbol{b} & \cdots & \sum_{i=1}^{P-M+1} O^{i-1}\boldsymbol{b} \end{bmatrix}_{6P\times 7M}$$

5.2 Optimisation Under Constraint

In the actual welding process, the displacement and speed of the joint and the end of the welding torch should be considered constraints in the optimiser design because of the limitations of the welding range, welding angle, servo motor configuration, and geometry of the gantry and robot arm.

First, the velocity constraint at the moment k is considered as follows:

$$\dot{\theta}_{\min} = \begin{bmatrix} L_{\min 1?} \\ L_{\min 2} \\ \dot{\theta}_{\min 1} \\ \vdots \\ \dot{\theta}_{\min 5} \end{bmatrix} \le \begin{bmatrix} L_{2?}(k) \\ L_2(k) \\ \dot{\theta}_1(k) \\ \vdots \\ \dot{\theta}_5(k) \end{bmatrix} \le \begin{bmatrix} L_{\max 1?} \\ L_{\max 2} \\ \dot{\theta}_{\max 1} \\ \vdots \\ \dot{\theta}_{\max 5} \end{bmatrix} = \dot{\theta}_{\max} \tag{9}$$

Therefore, this leads to a constraint on $U(k)$:

$$J \le DU \le K \tag{10}$$

where,

$$J = \begin{bmatrix} \dot{\theta}_{\min} \\ \vdots \\ \dot{\theta}_{\min} \end{bmatrix}_{7M\times 1}, K = \begin{bmatrix} \dot{\theta}_{\max} \\ \vdots \\ \dot{\theta}_{\max} \end{bmatrix}_{7M\times 1}, D = \begin{pmatrix} I & & \\ & \ddots & \\ & & I \end{pmatrix}_{7M\times 7M}.$$

Similarly, the constraint on the position at the moment k is obtained as follows:

$$S \le LU \le W \tag{11}$$

where,

$$S = \begin{bmatrix} \theta_{\min} \\ \vdots \\ \theta_{\min} \end{bmatrix}_{7M\times 1} - \begin{bmatrix} \theta(k-1) \\ \vdots \\ \theta(k-1) \end{bmatrix}_{7M\times 1},$$

$$W = \begin{bmatrix} \theta_{\max} \\ \vdots \\ \theta_{\max} \end{bmatrix}_{7M\times 1} - \begin{bmatrix} \theta(k-1) \\ \vdots \\ \theta(k-1) \end{bmatrix}_{7M\times 1},$$

$$L = \begin{bmatrix} T\cdot I & & \\ \vdots & \ddots & \\ T\cdot I & \cdots & T\cdot I \end{bmatrix}_{7M\times 7N}.$$

Finally, for welding operations, the process of weld-path planning is equivalent to obstacle avoidance. The author has described the trajectory of the simulated membrane wall welding process in Chapter 2, so the obstacle avoidance process is divided into a total of nine stages: AB, BC, CD, DE, EF, FG, GH, HI, and IJ, as shown in Figure 4.

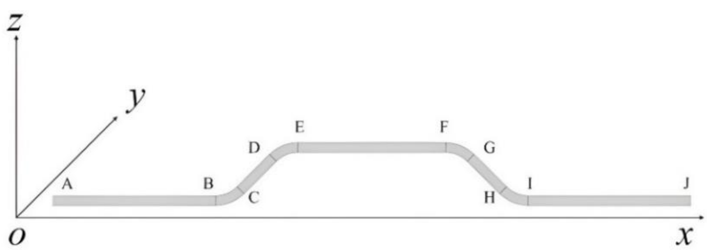

Figure 4 Movement Trajectories

During the operation of the welding torch, it was necessary to complete the obstacle avoidance operation. The mathematical model of an obstacle in welding tasks can be defined as:

$$ax + by + cz = d \tag{12}$$

The barrier can be set to (13):

$$\begin{cases} a_1 x^{(1)} + b_1 y^{(1)} + c_1 z^{(1)} > d_1 \\ a_2 x^{(2)} + b_2 y^{(2)} + c_2 z^{(2)} > d_2 \end{cases} \tag{13}$$

Then get the formula (14):

$$\begin{bmatrix} G_1 \\ G_2 \end{bmatrix} \cdot U(k) \le \begin{bmatrix} B_1 \\ B_2 \end{bmatrix} \tag{14}$$

where,

$$G_1 = \begin{pmatrix} T_1 & & \\ & \ddots & \\ & & T_1 \end{pmatrix}_{M\times 7M} G_y, T_1 = [D_1, D_2, \underbrace{0\cdots 0}_{5}]_{1\times 7}, \quad B_1 = -\begin{pmatrix} T_1 & & \\ & \ddots & \\ & & T_1 \end{pmatrix}_{M\times 7M} F_y x(k-1) - \begin{pmatrix} b_1 \\ \vdots \\ b_1 \end{pmatrix}$$

$$G_2 = \begin{pmatrix} T_2 & & \\ & \ddots & \\ & & T_2 \end{pmatrix}_{M\times 7M} G_y, \; T_2 = [0,0,\underbrace{\theta_4 \cdots \theta_8}_{5}]_{1\times 7}, \quad B_2 = -\begin{pmatrix} T_2 & & \\ & \ddots & \\ & & T_2 \end{pmatrix}_{M\times 7M} F_y x(k-1) - \begin{pmatrix} b_2 \\ \vdots \\ b_2 \end{pmatrix}$$

In conclusion, all the constraint conditions are defined as follows.

$$\begin{bmatrix} D \\ -D \\ L \\ -L \\ G_1 \\ G_2 \end{bmatrix} \boldsymbol{U}(k) \le \begin{bmatrix} K \\ -J \\ W \\ -S \\ B_1 \\ B_2 \end{bmatrix} \tag{15}$$

5.3 Dynamic Optimisation

The predictive control problem can be regarded as an optimisation issue. In essence, it involves calculating the M control inputs to bring outputs as close as possible to their desired values. Concurrently, it is imperative to ensure that variations in these inputs are gradual and controlled. Thus, we define the optimal problem as follows.

$$\min_{U(k)} J(k) = \| W(k) - Y(k) \|_Q^2 + \| U(k) \|_R^2 \tag{16}$$

$$s.t.\ Y(k) = F_y \cdot x(k) + G_y(k) \cdot U(k)$$

$$\begin{bmatrix} B \\ -B \\ D \\ -D \\ G_1 \end{bmatrix} U(k) \le \begin{bmatrix} H \\ -L \\ M \\ -N \\ W_1 \end{bmatrix} \tag{17}$$

where $W(k) = [w(k), \cdots, w(k+P)]^T$ is the expected output, Q is the output weighting matrix, and R is the control-weighting matrix.

We seek to minimise a quadratic cost function that encapsulates the discrepancy between the predicted and desired outputs, considering the smoothness of the control input transitions. This is achieved by adjusting the control weighting matrix R and the output weighting matrix Q, which are pivotal in balancing the trade-off between tracking performance and control effort.

Thus, the optimisation problem is transposed into a constrained quadratic programming problem, which is structured as follows:

$$\min_{U(k)} j(k) = \frac{1}{2} \boldsymbol{U}(k)^T \cdot H \cdot \boldsymbol{U}(k) + c \cdot \boldsymbol{U}(k)$$

$$s.t. \begin{bmatrix} B \\ -B \\ D \\ -D \\ G_1 \end{bmatrix} U(k) \le \begin{bmatrix} H \\ -L \\ M \\ -N \\ W_1 \end{bmatrix} \tag{18}$$

where,

$$H = 2\left(G_y(k)^T \boldsymbol{Q} G_y(k) + \boldsymbol{R}\right)$$
$$c = -2\left(W - F_y \cdot \boldsymbol{x}(k)^T \boldsymbol{Q} G_y(k)\right.$$

Subject to the constraints that regulate the control inputs, $U(k)$ is delineated by system-specific boundaries and limitations. Here, H represents a matrix that is a function of the control weighting matrix R, transposed output weighting matrix Q, and system dynamics, while c is a vector influenced by the difference between the target and predicted outputs, shaped by the output weighting matrix Q.

The optimal control inputs, that is, $U(k)$ are retrieved by resolving this quadratic programming dilemma. The selection of the function $\phi(k)$ for control is critical, as it ensures higher precision in position control than in speed control. This is accomplished by incorporating the system's previous state and control interval, resulting in the use of more precise control regulation rather than relying solely on it θ_k.

6 Results and Discussion

6.1 Experiments Description

The program consisted of two experiments: the MPC experiment simulated by MATLAB and the trajectory interpolation experiment simulated by CoppeliaSim and MATLAB. The specific content of the MPC experiment is to simulate the point-to-point motion trajectory to verify the correctness and feasibility of the algorithm, and the trajectory interpolation algorithm presents the welding process and the complexity of the whole experimental trajectory.

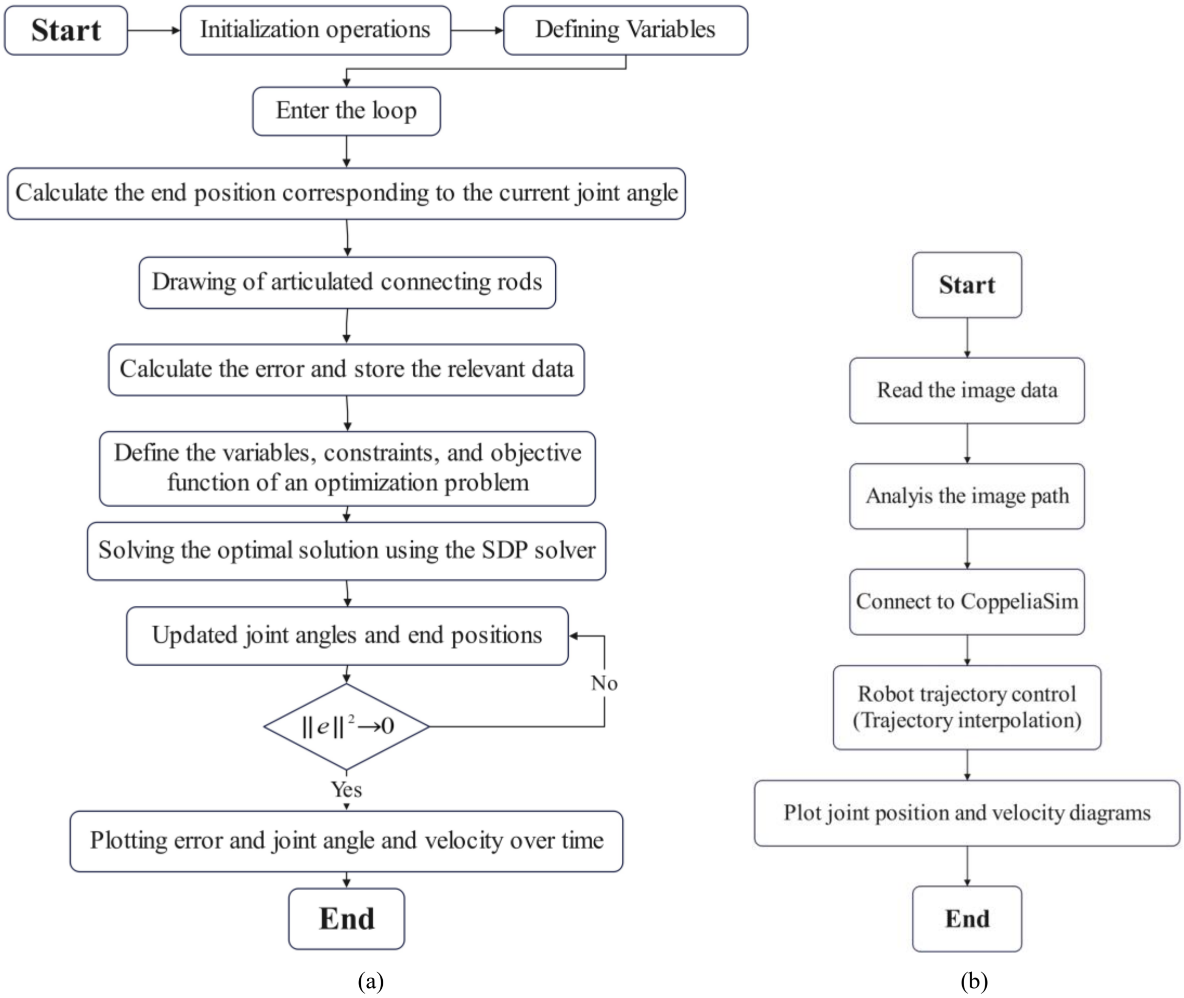

Figure 5 Experiment Description (a): MPC Experiment; (b): Trajectory Interpolation Experiment

MPC simulation: The program first performs initialisation operations such as clearing the workspace and closing the graph window. Subsequently, some variables are defined, such as the initial joint angle, target joint angle, error, and period. Subsequently, the program enters a loop, which is used to perform the joint angle optimisation calculation. In each loop, the program calculates the end position based on the current joint angle and plots a graph of the joint linkage. Next, the program calculates the error and stores relevant data. The program then uses the SDP solver to solve the optimal solution by defining the variables, constraints, and objective functions of the optimisation problem. Finally, the program updates the joint angles and end positions and performs the next loop. Simultaneously, the program plots the error, joint angle, and velocity over time to visualise the results.

Trajectory interpolation simulation: In the given code, the motion control module first extracts a predetermined trajectory from the image and then gradually controls the robot to move along this trajectory by interacting with the CoppeliaSim simulation environment. This process involves calculating the error between the current position and the target position and adjusting the robot's position and orientation according to this error and the set step size so that the robot gradually approaches or reaches the target position. In this code, the state flags in the loop indicate the state of the robot's motion: 1 for forward motion, 2 for reverse motion, 3 for forward lift, and 4 for stopped motion. In each loop, the code controls the robot to move to the target position, and adjusts the joint angles of the robot according to the target pose. A smooth, continuous trajectory was generated by interpolating discrete points on a given trajectory.

6.2 Analysis of Experimental Results and Performance Evaluation

Figure 6 shows an automated welding system for a gantry robotic arm in a CoppeliaSim simulation environment. The pink line in the figure indicates the running trajectory of the end of the welding torch, which was used to determine the precise movement trajectory of the robot during the welding process. This ensured the continuity and accuracy of the welding process.

The link to the experiment video is shown below: https://youtu.be/hNTd70lDDWY.

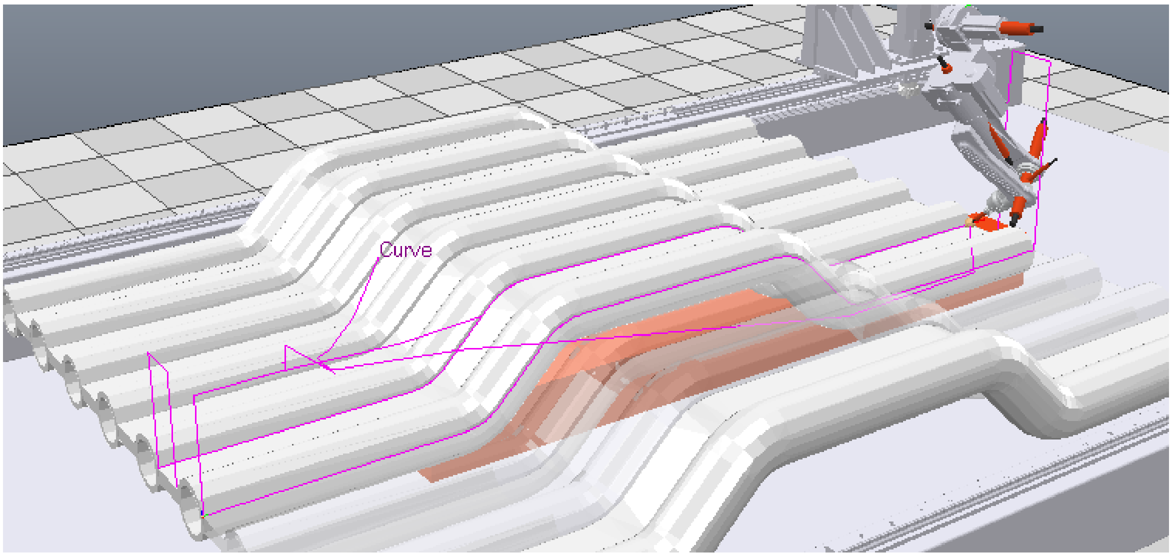

Figure 6 Torch end trajectory (Pink line)

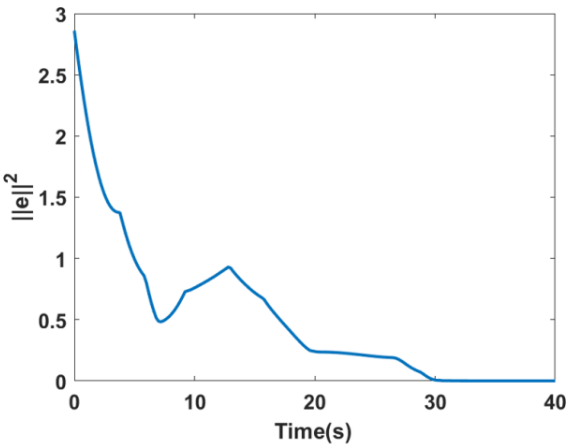

Figure 7 Convergence of Errors

Figure 7 shows the error trend between the spatial position at the end of the torch and the target point. First, the data show a clear downward trend, steadily decreasing from high values at the beginning of the experiment to lower stable values, which indicates the effectiveness of the MPC in the control of the robotic arm. During the initial phase (approximately 0–10 s), the fluctuations are very pronounced because the system is just starting to adjust or respond to some initial perturbation. There are several points of local minima throughout the motion, in particular, two points at approximately 15 s and 25 s, which may correspond to temporary stabilisation points of the system during the adjustment process. However, over time, the measurements stabilised, indicating that the system converged to a fixed point or steady state, and no significant outliers were found.

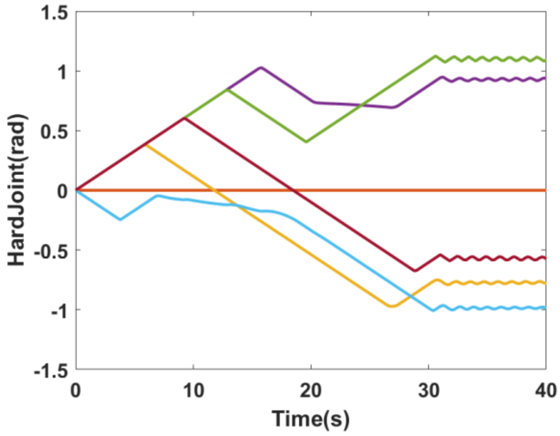

Figure 8 Angular Rotation of Robot Joints (MPC)

The trajectory tracking errors of the two-axis gantry and five-axis welding robot arm are shown in Figure 8. The errors of each axis showed different trends with time, indicating that the performance and response characteristics of each control axis may be different. The errors for some axes are small at the beginning of time, increase slightly, and then smooth or gradually decrease. This may indicate that the controller requires time to adapt or optimise the performance. At least two of the axes (axis1 and axis2) show a trend of decreasing errors over time, which suggests that MPC is effective in reducing trajectory tracking errors in these axes. Except for some fluctuations in the early stages, the errors in most axes seem to reach a steady state at approximately 35 seconds, which may indicate that the system has stabilised under MPC control.

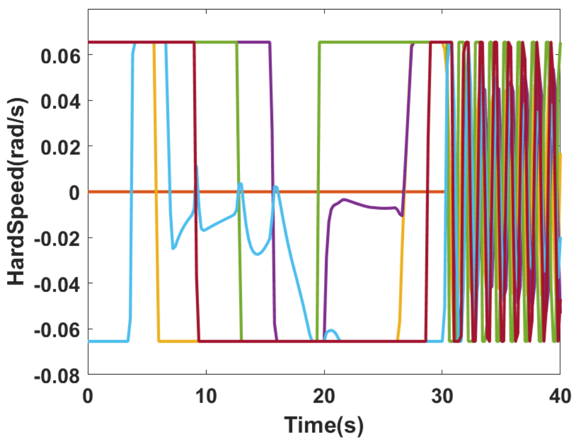

Figure 9 Angular Velocity Rotation of Robot Joints (MPC)

Figure 9 shows changes in control inputs or effects, and their sharp fluctuations on the timescale may indicate a sharp adjustment of the control action. At certain moments (e.g., approximately 10 and 30 s), spikes in the control inputs for multiple axes represent a temporary increase in intervention in the system, possibly correcting large trajectory deviations or responding to system perturbations. The control inputs appear to be very frequent and tight during the period of approximately 20 to 30 s, which may indicate that the control system is responding quickly to stabilise the system, or that the system is experiencing some complex dynamic problems during this time. Near the end of the graph (after approximately 35 seconds), the frequency and magnitude of the control inputs decreased significantly, indicating that the system may approach or reach the desired steady state.

The system shows adaptability to initial conditions and the ability to adjust to subsequent perturbations, particularly in the case of drastic changes in control inputs to correct trajectory errors. After a period of adjustment, the system appears to stabilise, suggesting that the MPC algorithm successfully steers the system to a more stable operating state. The high-frequency fluctuations in the control inputs, on the other hand, may indicate that the control strategy may need to be further optimised to reduce consumption and improve the overall efficiency of the system.

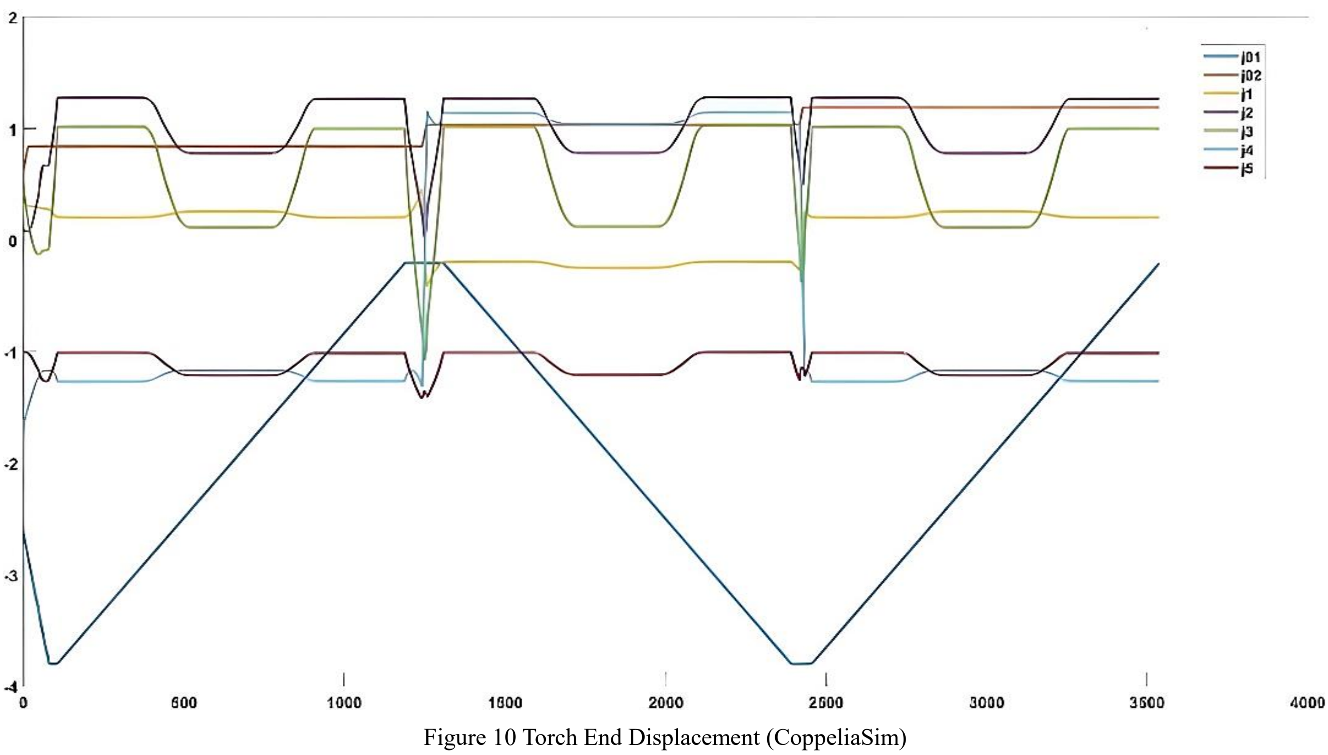

Figure 10 Torch End Displacement (CoppeliaSim)

Figure 10 shows the positions of the different joints over time, and the position of each joint changes in steps, indicating that motion is controlled by the MPC algorithm. At some points in time, especially around 1000 and 2500, the positions of all joints change almost simultaneously. This reflects the synergistic motion of the gantry and the robotic arms. After each step, the position line is mostly flat, which indicates that the joints hold their positions stably without significant overshoot or oscillation, which suggests that the control system is stable. All joints showed significant peaks at approximately 1000 and 2500 time points. From Figure 4. Movement Trajectories, the main reason for this peak is the uphill and downhill processes of "BE" and "FI."

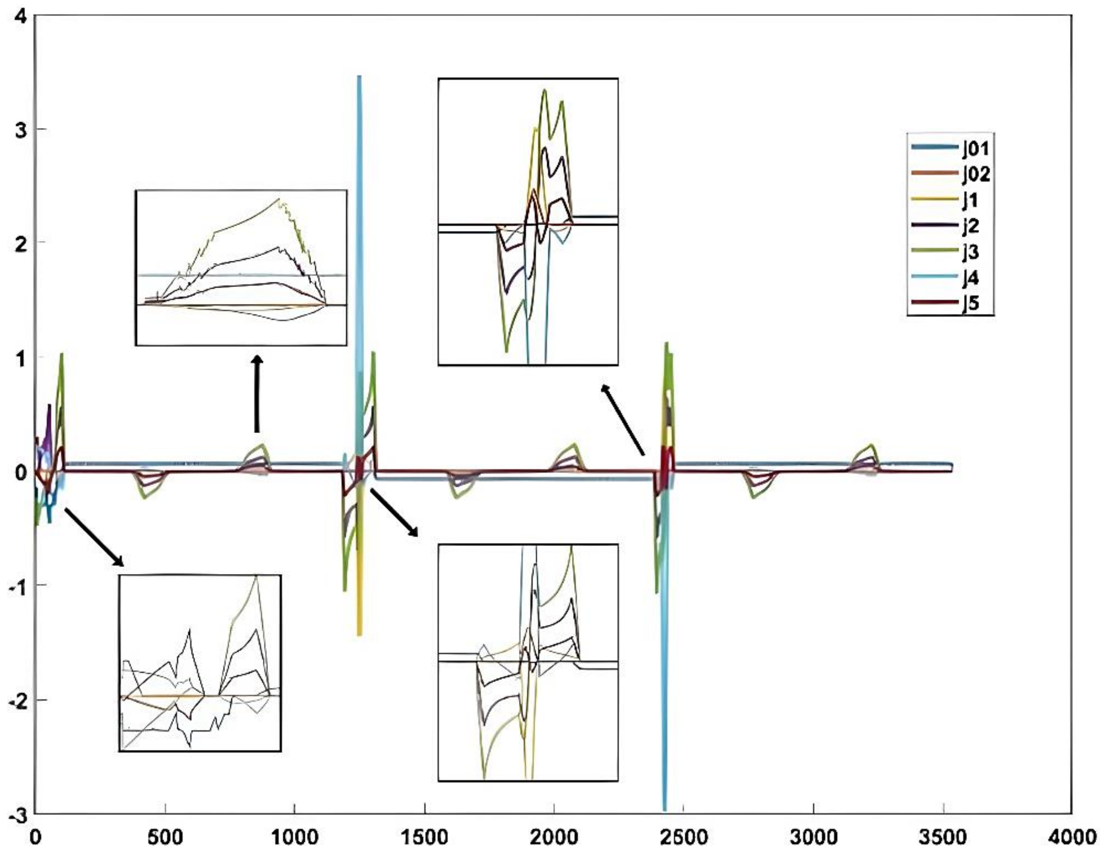

Figure 11 Torch End Velocity (CoppeliaSim)

Figure 11 where represents the velocity of each joint during the same period. Firstly, it can be seen that the flat line of zero velocity correlates with the flat line of the joint position graph, indicating that the joints did not move during this period and maintained their positions. The spikes, which correspond to the steps in the position graph, indicate a rapid change in position and, therefore, higher velocities. The spikes should match the rate of change in the position map. Similar to the position map, the spikes in velocity, particularly the large spikes around the 1000 and 2500 time points, exemplify the effect of changes in the spatial structure of the weld on the stability of the path-tracking algorithm.

Synchronisation of these motions across all joints suggests a coordinated control strategy when the membrane wall welding platform performs a complex path or task, reflecting the superiority and necessity of the gantry robotic arm structure for complex spatial path tracking tasks.

7 Conclusion

The present study demonstrates the efficacy of Model Predictive Control (MPC) in trajectory tracking of membrane wall welding using a gantry robotic arm. The study demonstrates that MPC offers a more efficient and accurate control scheme with its prediction and optimisation capabilities. The simulation experiments conducted in CoppeliaSim and MATLAB demonstrate the MPC's proficiency in managing complex multi-stage welding tasks, efficiently handling multiple inputs and outputs, and considering system constraints. Nonetheless, the study also revealed some challenges, such as controlling fluctuations and spikes in the outputs, which may arise in response to trajectory errors or external disturbances. These issues highlight the need to optimise MPC parameters further and control strategies to enhance energy efficiency and ensure smooth operation.

Conflicts of Interest

The authors declare no competing interests.

References

[1] Sun, D.-S., Lee, T.-E. & Kim, K.-H. (2005) Component allocation and feeder arrangement for a dual-gantry multi-head surface mounting placement tool. International Journal of Production Economics. 95(2), 245-264. https://doi.org/10.1016/j.ijpe.2004.01.003

[2] Wang, X., Xie, Z., Zhou, X., Gao, J., Li, F. & Gu, X. (2022) Adaptive path planning for the gantry welding robot system. Journal of Manufacturing Processes. 81, 386-395. https://doi.org/10.1016/j.jmapro.2022.07.005

[3] Wenna, W., Weili, D., Changchun, H., Heng, Z., Haibing, F. & Yao, Y. (2022) A digital twin for 3D path planning of large-span curved-arm gantry robot. Robotics and Computer-Integrated Manufacturing. 76, 102330. https://doi.org/10.1016/j.rcim.2022.102330

[4] Yang, X., Hu, H. & Cheng, C. (2023) Flexible yard space allocation plan for new type of automated container terminal equipped with unilateral-cantilever rail-mounted gantry cranes. Advanced Engineering Informatics. 58, 102193. https://doi.org/10.1016/j.aei.2023.102193

[5] Wang, X., Zhou, X., Xia, Z. & Gu, X. (2021) A survey of welding robot intelligent path optimization. Journal of Manufacturing Processes. 63, 14-23. https://doi.org/10.1016/j.jmapro.2020.04.085

[6] Wen, D., Yao, Y. S., Li, L., Jeon, M.-G., Zhou, Q. L., Li, N. & Deguchi, Y. (2019) Experimental study on the working states of membrane walls in the arch-fired boiler with different fuel proportion coefficients. Applied Thermal Engineering. 148, 404-411. https://doi.org/10.1016/j.applthermaleng.2018.10.098

[7] Yang, A., Chen, Y., Naeem, W., Fei, M. & Chen, L. (2021) Humanoid motion planning of robotic arm based on human arm action feature and reinforcement learning. Mechatronics. 78, 102630. https://doi.org/10.1016/j.mechatronics.2021.102630

[8] Kumar, S. A., Chand, R., Chand, R. P. & Sharma, B. (2023) Linear manipulator: Motion control of an *n*-link robotic arm mounted on a mobile slider. Heliyon. 9(1). https://doi.org/10.1016/j.heliyon.2023.e12867

[9] Golovin, I., Maksakov, A., Shysh, M. & Palis, S. (2022) Discrepancy-based control for positioning of large gantry crane. Mechanical Systems and Signal Processing. 163, 108199. https://doi.org/10.1016/j.ymssp.2021.108199

[10] Ji, X., Chen, Y. & Yang, S. (2022) Stud welding system using an industrial robot for membrane walls. The International Journal of Advanced Manufacturing Technology. 121(11), 8467-8477. https://doi.org/10.1007/s00170-022-09892-9

[11] Taysom, B. S., Sorensen, C. D. & Hedengren, J. D. (2017) A comparison of model predictive control and PID temperature control in friction stir welding. Journal of Manufacturing Processes. 29, 232-241. https://doi.org/10.1016/j.jmapro.2017.07.015

[12] Ma, L., Lou, X. & Jia, J. (2023) Neural-network-based boundary control for a gantry crane system with unknown friction and output constraint. Neurocomputing. 518, 271-281. https://doi.org/10.1016/j.neucom.2022.11.010

[13] Wang, X., Gao, J., Zhou, X. & Gu, X. (2024) Path Planning for the Gantry Welding Robot System Based on Improved RRT*. Robotics and Computer-Integrated Manufacturing. 85, 102643. https://doi.org/10.1016/j.rcim.2023.102643

[14] Awad, N., Lasheen, A., Elnaggar, M. & Kamel, A. (2022) Model predictive control with fuzzy logic switching for path tracking of autonomous vehicles. ISA Transactions. 129, 193-205. https://doi.org/10.1016/j.isatra.2021.12.022

[15] Liu, Z., Chang, G., Yuan, H., Tang, W., Xie, J., Wei, X. & Dai, H. (2023) Adaptive look-ahead model predictive control strategy of vehicular PEMFC thermal management. Energy. 285, 129176. https://doi.org/10.1016/j.energy.2023.129176

[16] Schwenzer, M., Ay, M., Bergs, T. & Abel, D. (2021) Review on model predictive control: an engineering perspective. The International Journal of Advanced Manufacturing Technology. 117(5), 1327-1349. https://doi.org/10.1007/s00170-021-07682-3

[17] Brian Froisy, J. (1994) Model predictive control: Past, present and future. ISA Transactions. 33(3), 235-243. https://doi.org/10.1016/0019-0578(94)90095-7

[18] Lv, C., Wang, G. & Chen, H. (2020) Estimation of time-dependent thermal boundary conditions and online reconstruction of transient temperature field for boiler membrane water wall. International Journal of Heat and Mass Transfer. 147, 118955. https://doi.org/10.1016/j.ijheatmasstransfer.2019.118955

[19] Zhang, Z., Malashkhia, L., Zhang, Y., Shevtshenko, E. & Wang, Y. (2022) Design of Gaussian process based model predictive control for seam tracking in a laser welding digital twin environment. Journal of Manufacturing Processes. 80, 816-828. https://doi.org/10.1016/j.jmapro.2022.06.047

[20] García, C. E., Prett, D. M. & Morari, M. (1989) Model predictive control: Theory and practice—A survey. Automatica. 25 (3), 335-348. https://doi.org/10.1016/0005-1098(89)90002-2

[21] Qin, S. J. & Badgwell, T. A. (2003) A survey of industrial model predictive control technology. Control Engineering Practice. 11(7), 733-764. https://doi.org/10.1016/S0967-0661(02)00186-7

[22] Lancaster, J. F. (1973) Failures of boilers and pressure vessels: Their causes and prevention. International Journal of Pressure Vessels and Piping. 1(2), 155-170. https://doi.org/10.1016/0308-0161(73)90020-3